Electronic Supplementary Material (ESI) for Nanoscale Advances.

Solvent-driven crystal-crystal transformation and morphology change in a 2D layer inorganic POM-based framework

Hui-Min Zeng, Chao Wang, Wei-Hong Wu, Wei-Tao Mao, Zhan-Guo Jiang*, Cai-Hong Zhan*

Table of Contents

S1 Materials

All the chemicals, whether regents or solvent, were purchased from suppliers and used as received without further purification. Molybdenum trioxide (MoO_3, 99.5%) were purchased from Aladdin. Sodium hydroxide (NaOH, AR), Nitric acid (HNO_3, AR) Manganese nitrate 50% aqueous solution ($Mn(NO_3)_2$) and all kinds of organic solvents were purchased from Sinopharm Chemical Reagent Co., Ltd., China.

S2 General Experimental Section

Powder X-ray Diffraction (PXRD)

Powder XRD patterns were recorded on a Bruker D8 Advance X-ray diffractometer with (λ (CuKα) = 1.5405 Å) radiation in the 2θ range of 5-50°.

Fourier Transform Infrared Spectroscopy (FTIR)

FTIR Spectroscopy (KBr pellets) were obtained from a Nicolet NEXUS 670 spectrometer in the range of 400 and 4000 cm^{-1}.

Thermogravimetric Analyses (TGA)

Thermogravimetric Analyses were carried out under N_2 atmosphere on a TA Instruments STA499 F5 thermobalance at the rate of 10 ℃/min heating from 20 ℃ to 800 ℃.

Elemental Analyses (EA)

H microanalyse was performed on a Perkin-Elmer 240C elemental analyser, and ICP-OES analyses were carried out on a PerkinElmer Optima 8300 optical emission spectrometer.

UV-Vis spectrophotometer (UV)

UV-Vis absorption spectra were acquired on a Carry 5000 spectrophotometer, in which the range of wavenumber was setted at 300 to 800 nm.

Impedance spectroscopy (EIS)

The electrochemical impedance spectroscopy (EIS) measurement was performed on the CHI760E electrochemical workstation at room temperature and carried out by applying an AC voltage with 10 mV amplitude over a frequency range from 0.1 Hz to 100 kHz.

SEM Measurements

Scanning electron microscopy (SEM) measurement was carried out using S-4800.

Single-crystal X-ray diffraction (SCXRD)

Single-crystal X-ray diffraction data collection of compound 1 and 1a were recorded on Bluker D8 VENTURE diffractometer equipped with a PHOTON 100 CMOS bidimensional detector and MoKα monochromatized radiation (λ = 0.71073 Å) at 150 K. The structure of target compounds was solved by intrinsic phasing methods and refined by full-matrix least squares using the SHELX-TL package[1]. All of the non-hydrogen atoms are dealt with anisotropic thermal parameters. Hydrogen atoms on water are not identified. Further details about of the crystal structure determinations may be obtained free of charge via the Internet at https://www.ccdc.cam.ac.uk/ CCDC 2023819, 2060052. Crystallographic data for single-crystal X-ray diffraction studies are summarized in Table S1.

S3 Synthesis and Experimental Section

Synthesis of 1 $Na_6(MnMo_8O_{28}) \cdot (H_2O)_{19}$

The pH value of the aqueous solution of molybdenum trioxide (2.8788 g, 20 mmol) and sodium hydroxide (1.6 g, 40 mmol) dissolved in H_2O (20 mL) was adjusted to 4.0 by adding nitric acid. Then 2 mL above solution were taken out into 10 mL glass vial, then 100 μL manganese nitrate 50% aqueous solution were added with vigorous stirring. The clear yellow solution was allowed to evaporate in an open vial at room temperature. After two days, yellow rod crystal was obtained and collected by filtration and air-dried. Yield: 17.7 % based on Mo. FT-IR spectrum of **1** is given in Fig. S11. Elemental analysis: Calc. (found): H 2.1 (2.0); Mo 43.8 (42.5); Na 7.9 (8.2); Mn 3.1 (2.9). TGA (Fig. S26) showed a weight loss of 19 % in the 20-150 °C temperature range corresponding to the 19 hydration water.

Synthesis of 1a $Na_6(MnMo_8O_{28}) \cdot (H_2O)_8$

Compound 1 was soaked in acetone for 3h, yellow rod crystal was obtained and collected by filtration and air-dried. Yield: 17.7 % based on Mo. FT-IR spectrum of **1** is given in Fig. S11. Elemental analysis: Calc. (found): H 2.0 (2.5); Mo 44.7 (45.5); Na 8.0 (7.8); Mn 3.4 (3.6). TGA (Fig. S26) showed a weight loss of 10.4 % in the 20-150 °C temperature range corresponding to the 8 hydration water.

S4 Crystal data and structure refinement

Table S1. Crystal data and structure refinement for Compound 1 and Compound 1a.

Empirical formula	$MnMo_8Na_6O_{47}$	Empirical formula	$MnMo_8Na_6O_{38}$
Formula weight	1712.40	Formula weight	1568.40
Temperature/K	150	Temperature/K	295(2)
Crystal system	triclinic	Crystal system	triclinic
Space group	P-1	Space group	P-1
a/Å	9.5413(5)	a/Å	8.4167(6)
b/Å	9.8153(5)	b/Å	9.5106(6)
c/Å	11.6931(6)	c/Å	10.0211(7)
α/°	103.743(2)	α/°	90.941(2)
β/°	101.067(2)	β/°	100.403(2)
γ/°	95.735(2)	γ/°	105.123(2)
Volume/$Å^3$	1031.70(9)	Volume/$Å^3$	759.95(9)
Z	1	Z	1
$\rho_{calc}g/cm^3$	2.756	$\rho_{calc}g/cm^3$	3.427
μ/mm^{-1}	2.834	μ/mm^{-1}	3.810
F(000)	803	F(000)	731.0
Crystal size/mm^3	0.2 × 0.2 × 0.1	Crystal size/mm^3	0.3 × 0.1 × 0.1
Radiation	MoKα (λ = 0.71073)	Radiation	MoKα (λ = 0.71073)
2Θ range for data collection/°	4.402 to 55.03	2Θ range for data collection/°	4.446 to 54.782
Index ranges	$-12 \le h \le 12$, $-12 \le k \le 11$, $-14 \le l \le 15$	Index ranges	$-10 \le h \le 10$, $-11 \le k \le 12$, $-12 \le l \le 12$
Reflections collected	11677	Reflections collected	7857
Independent reflections	4705 [R_{int} = 0.0170, R_{sigma} = 0.0216]	Independent reflections	3409 [R_{int} = 0.0242, R_{sigma} = 0.0348]
Data/restraints/parameters	4705/2/278	Data/restraints/parameters	3409/0/244
Goodness-of-fit on F^2	1.115	Goodness-of-fit on F^2	1.155
Final R indexes [I>=2σ (I)]	R_1 = 0.0393, wR_2 = 0.1094	Final R indexes [I>=2σ (I)]	R_1 = 0.0475, wR_2 = 0.1199
Final R indexes [all data]	R_1 = 0.0416, wR_2 = 0.1173	Final R indexes [all data]	R_1 = 0.0588, wR_2 = 0.1341
Largest diff. peak/hole / e $Å^{-3}$	4.48/-1.89	Largest diff. peak/hole / e $Å^{-3}$	2.18/-1.70

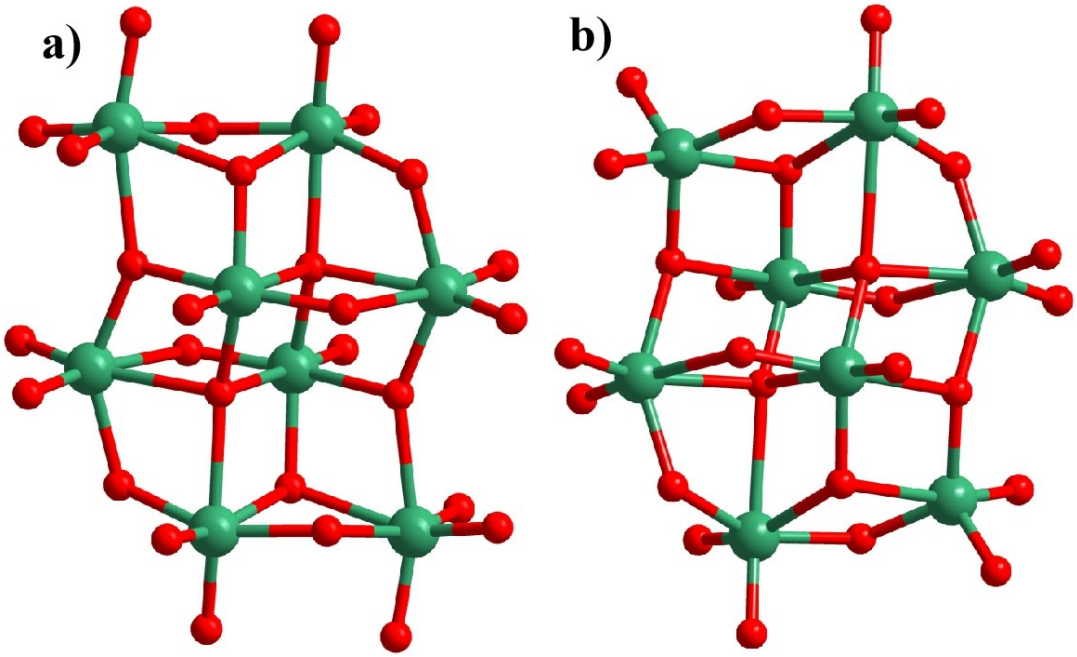

Fig. S1 Ball-and-stick representations for the {Mo_8} unit, (a) for {Mo_8O_{28}} and (b) for {Mo_8O_{26}}. color codes (the same in the following picture): Mo, green; O, red.

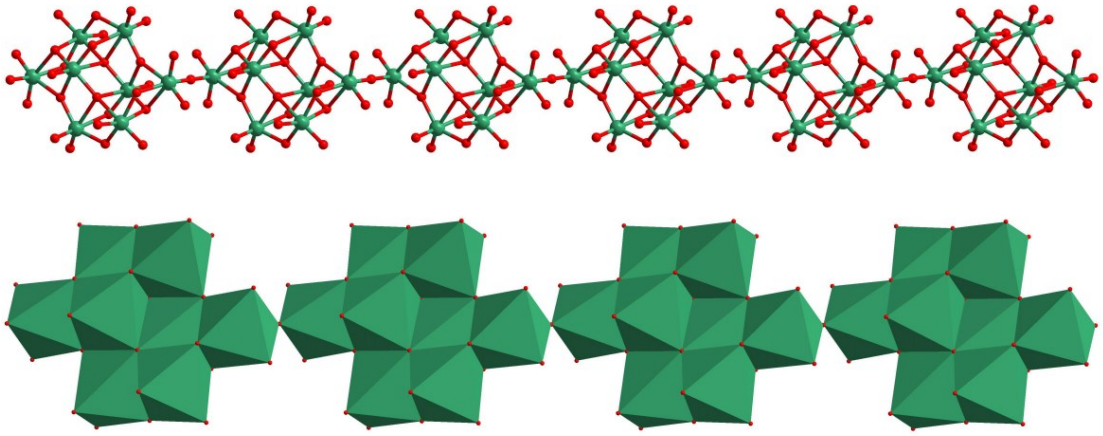

Fig. S2 Ball-and-stick and polyhedral representations for a 1D infinite vertex-shared {γ-Mo_8O_{28}} chain.

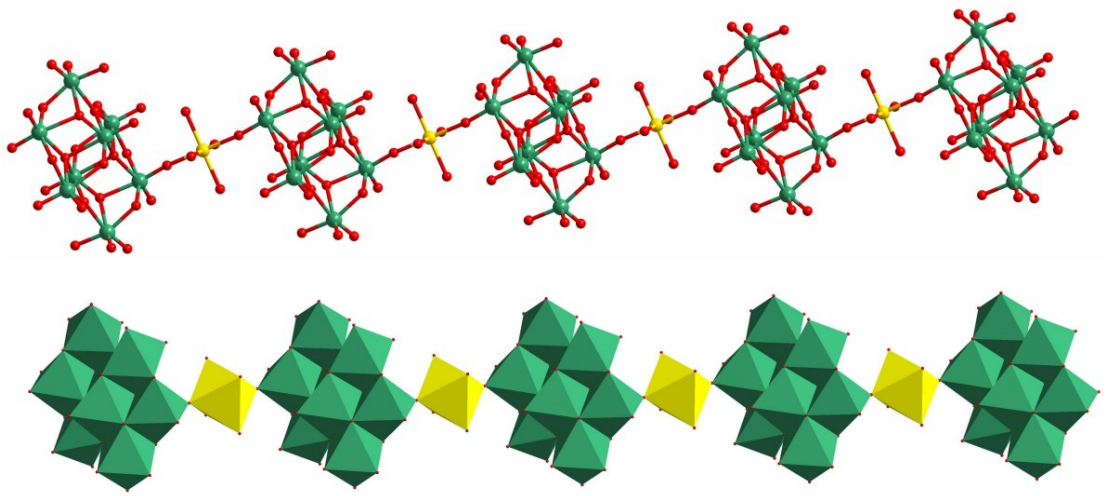

Fig. S3 Ball-and-stick and polyhedral representations for a 1D infinite chain.

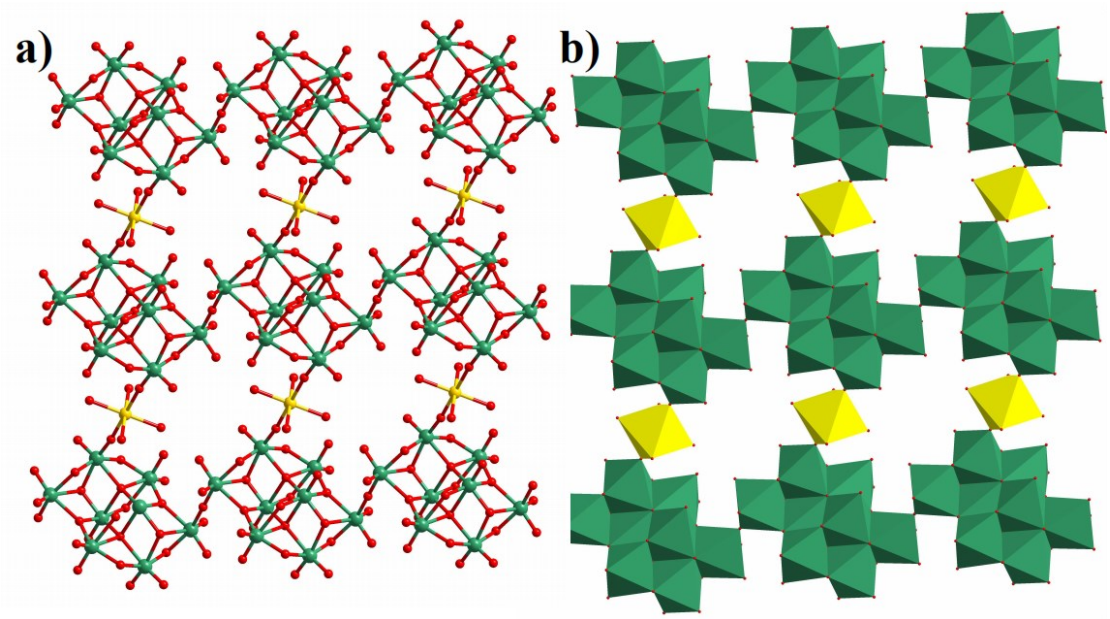

Fig. S4 (a) Ball and stick presentation of the 2D $\{MnMo_8O_{28}\}_n$ sheet. (b) Polyhedral presentation of the 2D $\{MnMo_8O_{28}\}_n$ sheet. (MoO_6 octahedra, green; MnO_6 octahedra, yellow).

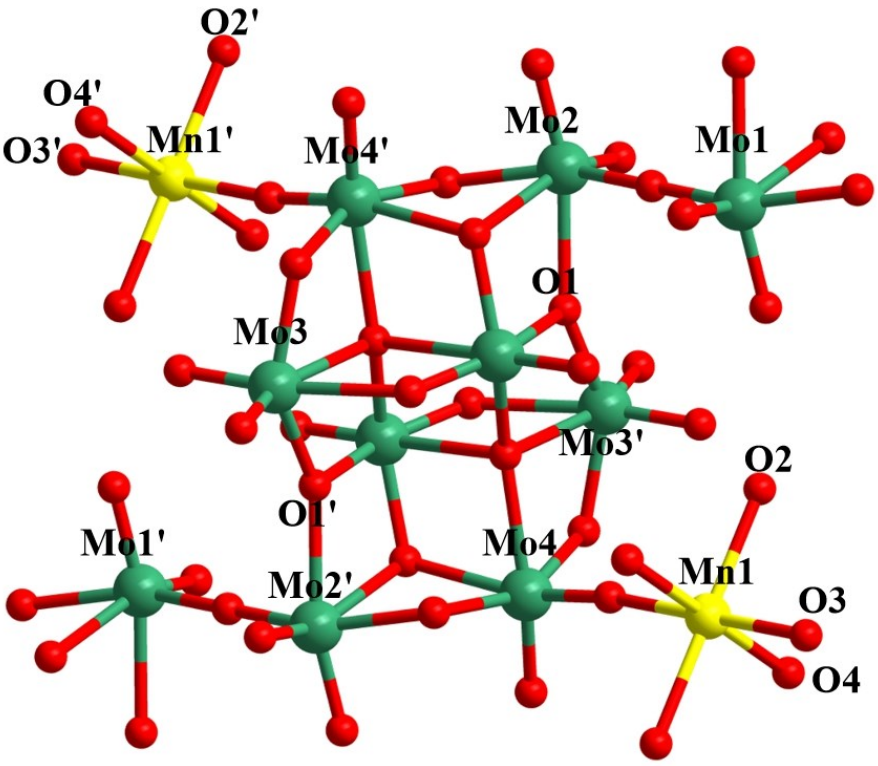

Fig. S5 Ball and stick presentation for the $\{Mo_8\}$ unit with two Mn and Mo linkers in one layer.

Table S2. Distances (Å) comparison between corresponding atoms in Compound 1 and Compound 1a as demonstrated in Figure S5.

	Compound 1	Compound 1a
Mo1-Mo2	3.7987	3.7673
Mo3-O1	4.9414	4.9340
Mo4-Mn1	3.8502	3.8438
Mo4-Mo2'	3.2989	3.2986
Mn1-O2	2.1865	2.2026
Mn1-O3	2.1191	2.1236
Mn1-O4	2.2103	2.2086

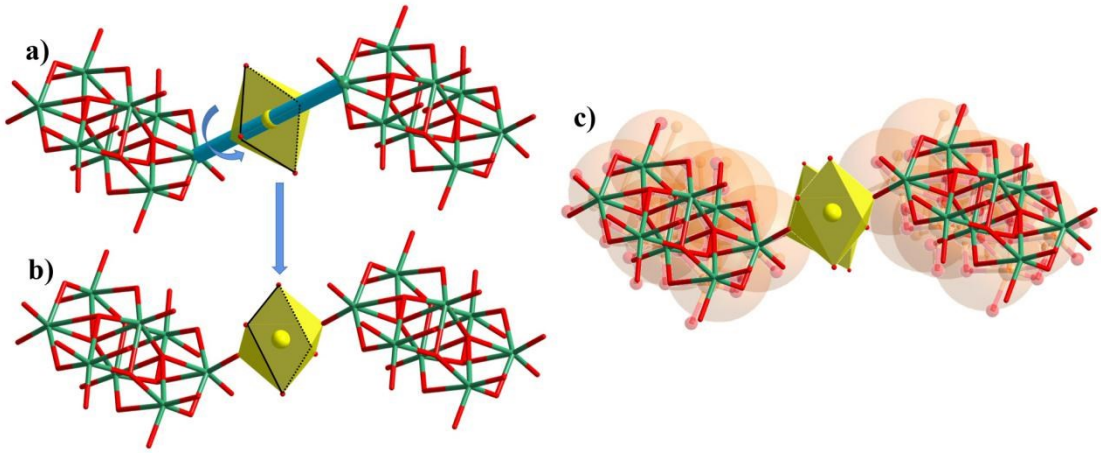

Fig. S6 Ball and stick presentation for two $\{Mo_8\}$ unit with one $\{MnO_6\}$ octahedron of Compound 1 (a) and Compound 1a (b); (c) Compound 1 and Compound 1a superimposed together.

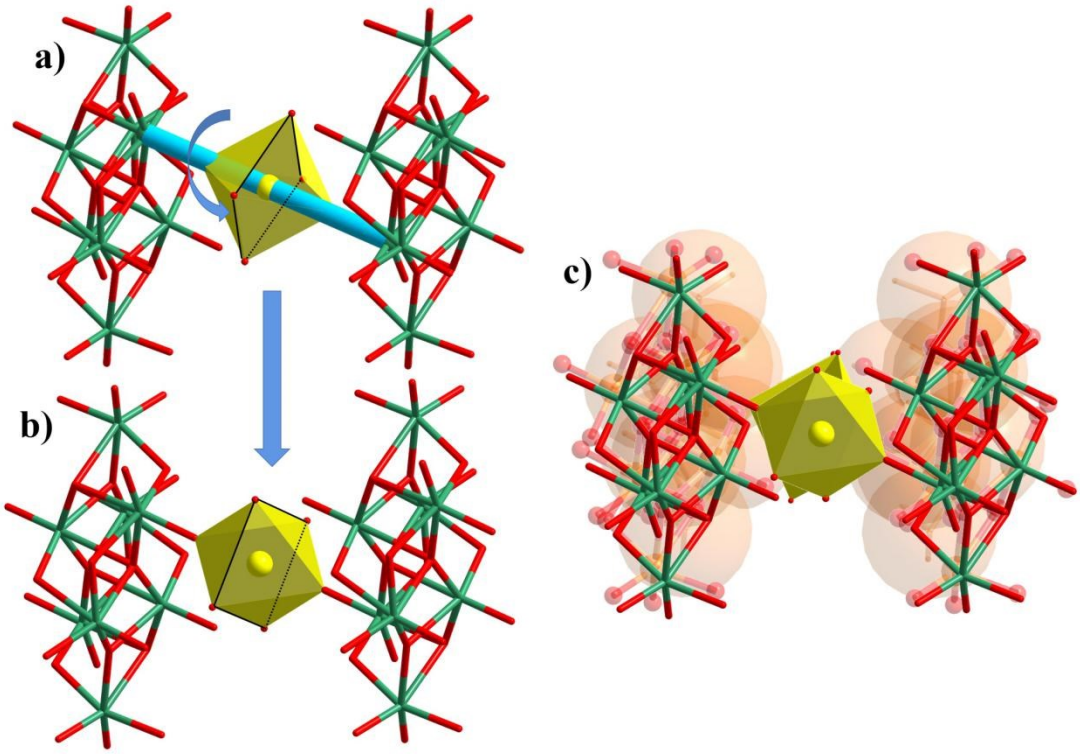

Fig. S7 Ball and stick presentation for two $\{Mo_8\}$ unit with one $\{MnO_6\}$ octahedron of Compound 1 (a) and Compound 1a (b); (c) Compound 1 and Compound 1a superimposed together.

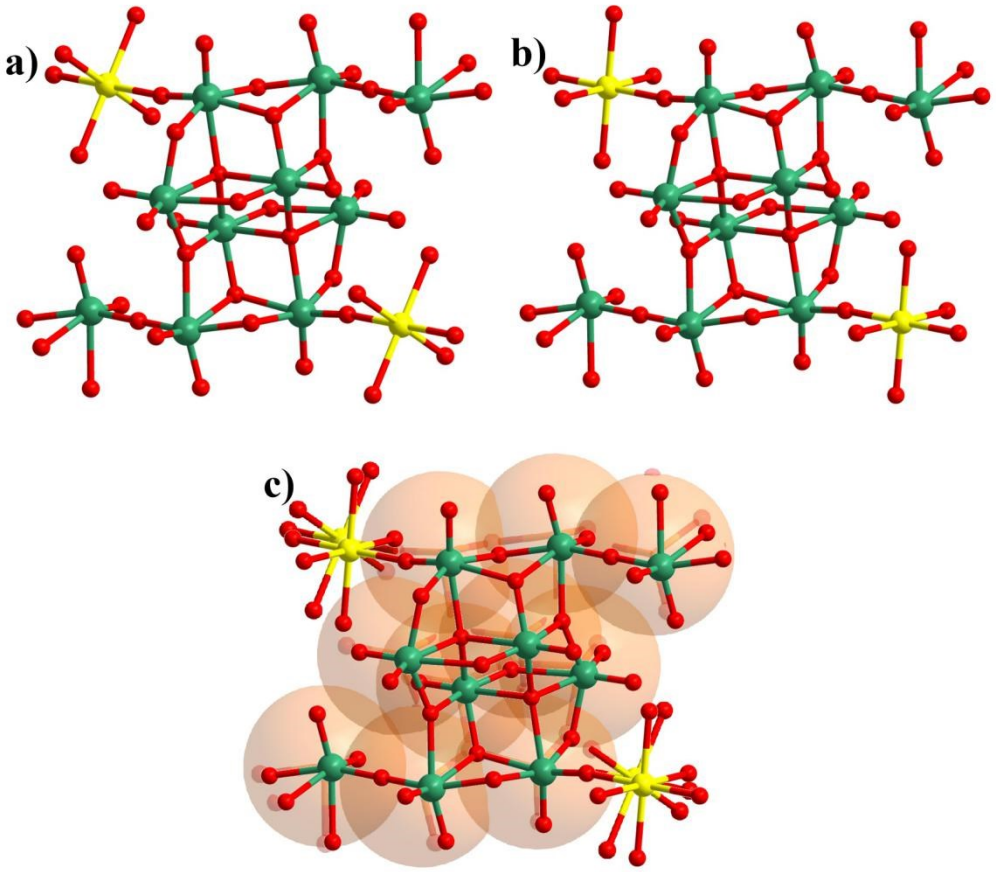

Fig. S8 Ball and stick presentation for two {Mo_8} unit with one two Mn and Mo linkers of Compound 1 (a) and Compound 1a (b); (c) Compound 1 and Compound 1a superimposed together.

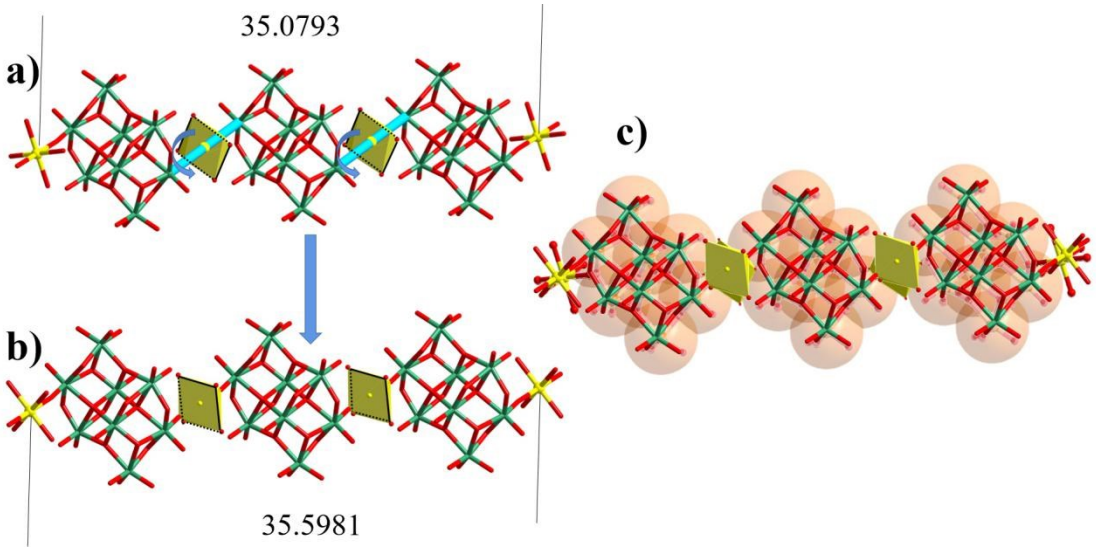

Fig. S9 Ball and stick presentation for 1D infinite chain of Compound 1 (a) and Compound 1a (b); (c) Compound 1 and Compound 1a superimposed together.

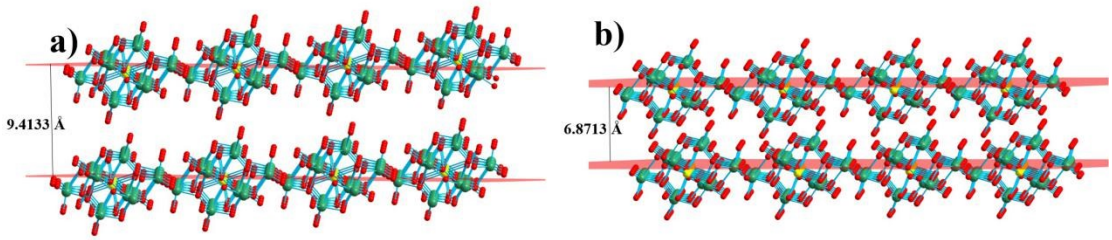

Fig. S10 Stacking of the 2D network structure of Compound 1 (a) and Compound 1a (b).

S5 Fourier Transform Infrared Spectroscopy (FTIR)

The IR spectrum of Compound 1 and 1a are showed in the Fig. S11, the band at 3400 cm^{-1}, 1630 cm^{-1} for 1 and 3410 cm^{-1}, 1630 cm^{-1} for 1a correspond to asymmetric stretching vibration of υ_{as} (H_2O) and δ (H_2O) deformation vibrations respectively. The characteristic absorb band in the range of 900 cm^{-1} to 500 cm^{-1} belongs to Mo-O bond, in which 943 cm^{-1} for 1, 945 cm^{-1} for 1a are attributed to υ ($Mo_{=}O_t$) vabaration respectively.

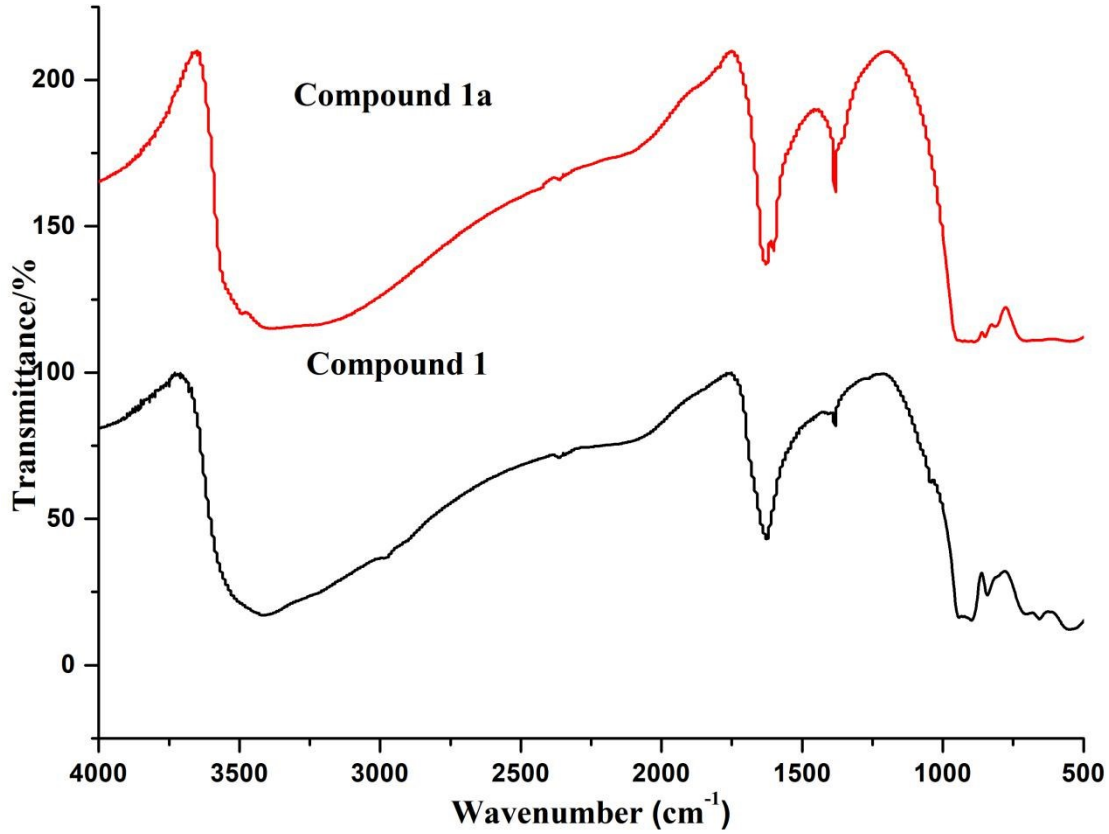

Fig. S11 FT-IR spectra of Compound 1 (black) and Compound 1a (red).

S6 Powder X-ray diffraction (PXRD)

The powder X-ray diffraction (PXRD) patterns for Compound 1 can be compared with the simulated pattern obtained from the X-ray single-crystal diffraction analysis. Their peak positions are in good agreement with each other, indicating the phase purity of the product. The differences in intensity may be due to the preferred orientation of the powder sample.

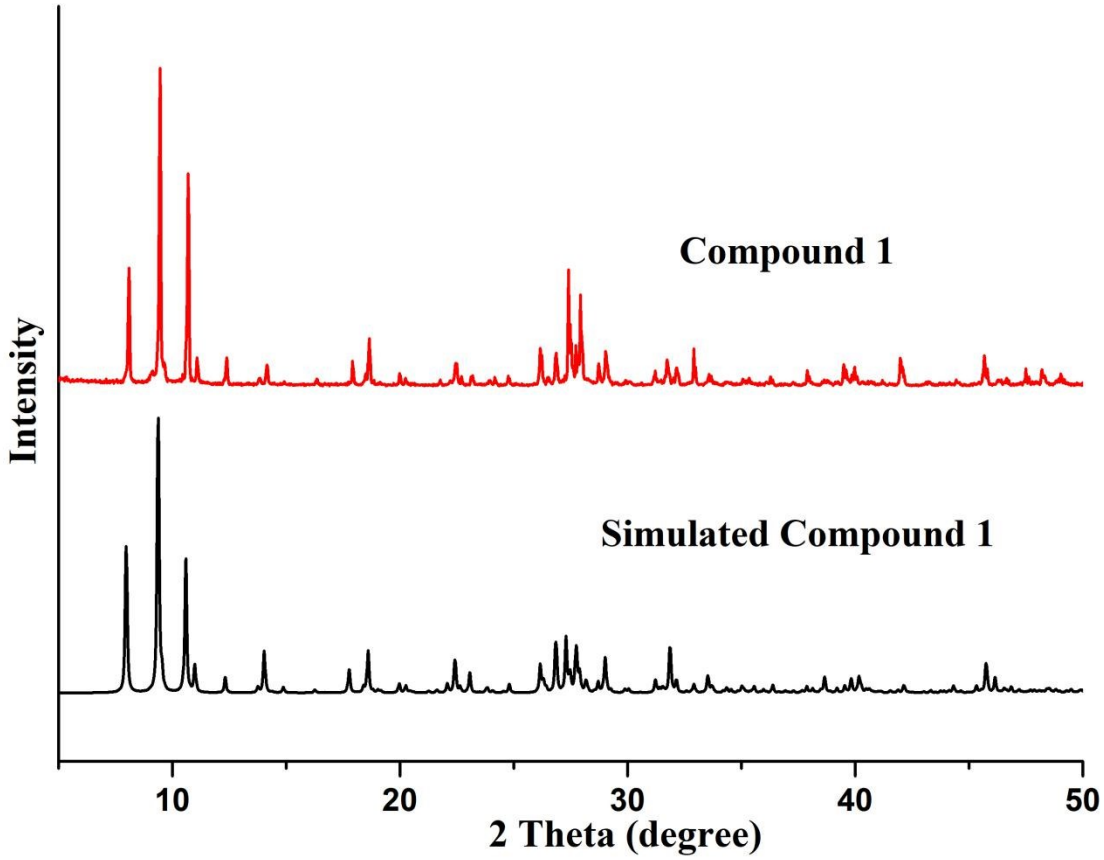

Fig. S12 Experimental (red, Compound 1) and simulated (black) PXRD patterns.

Fig. S13 The graph of Compound 1 died under the air condition (left) and vacuum condition (right).

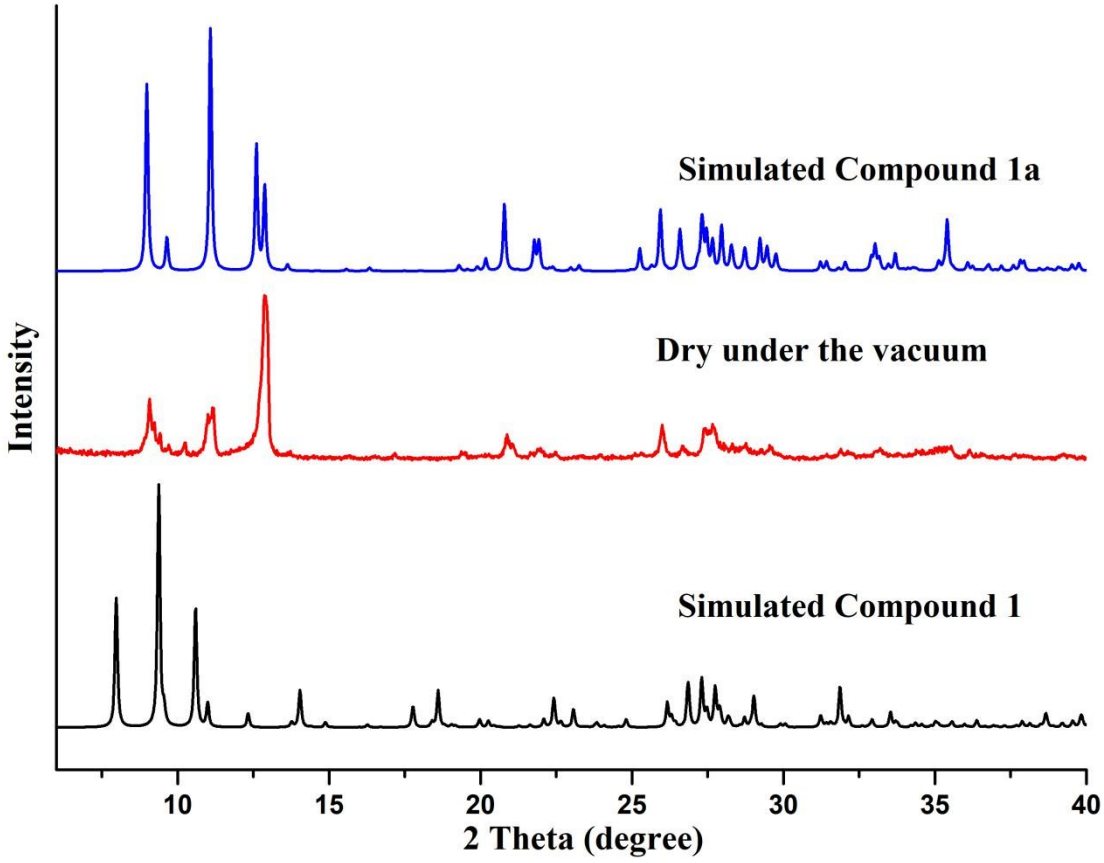

Fig. S14 Experimental (red, dry under the vacuum) and simulated (black for Compound 1, blue for Compound 1a) PXRD patterns.

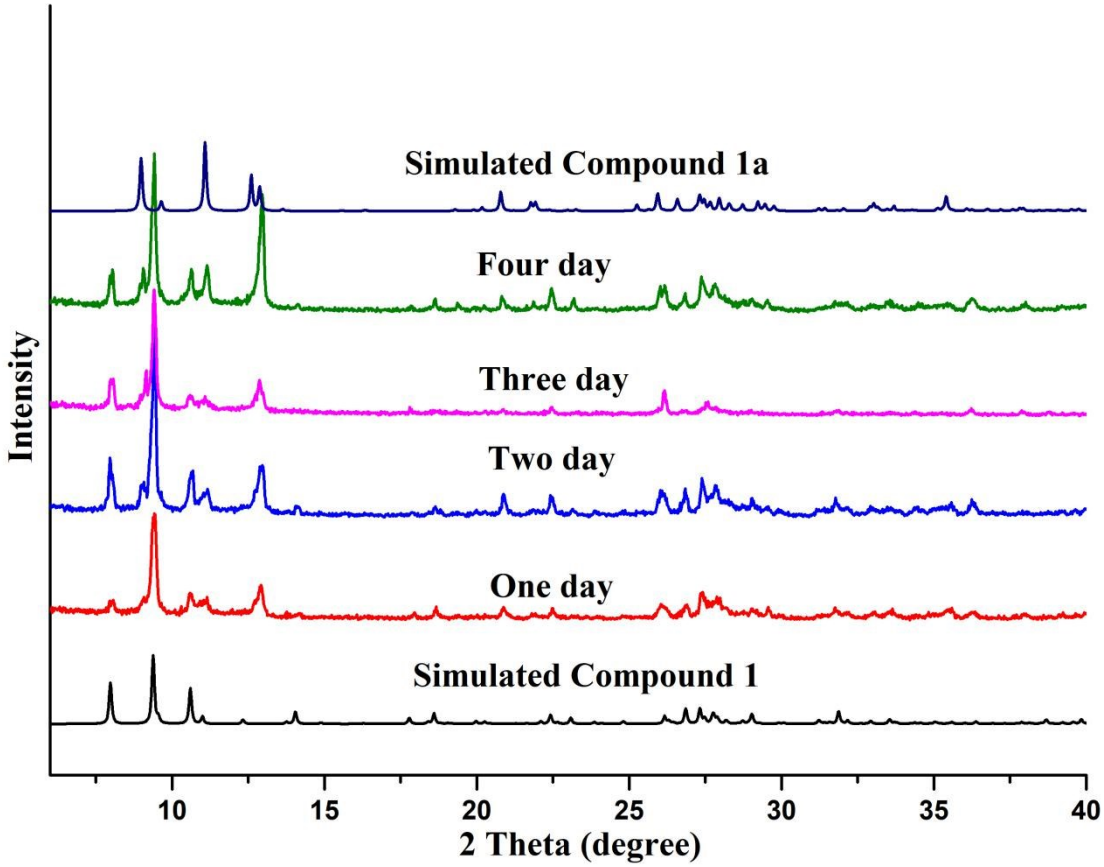

Fig. S15 Time-dependent PXRD patterns of Compound 1 soaked in ether and simulated (black for Compound 1, dark blue for Compound 1a) PXRD patterns.

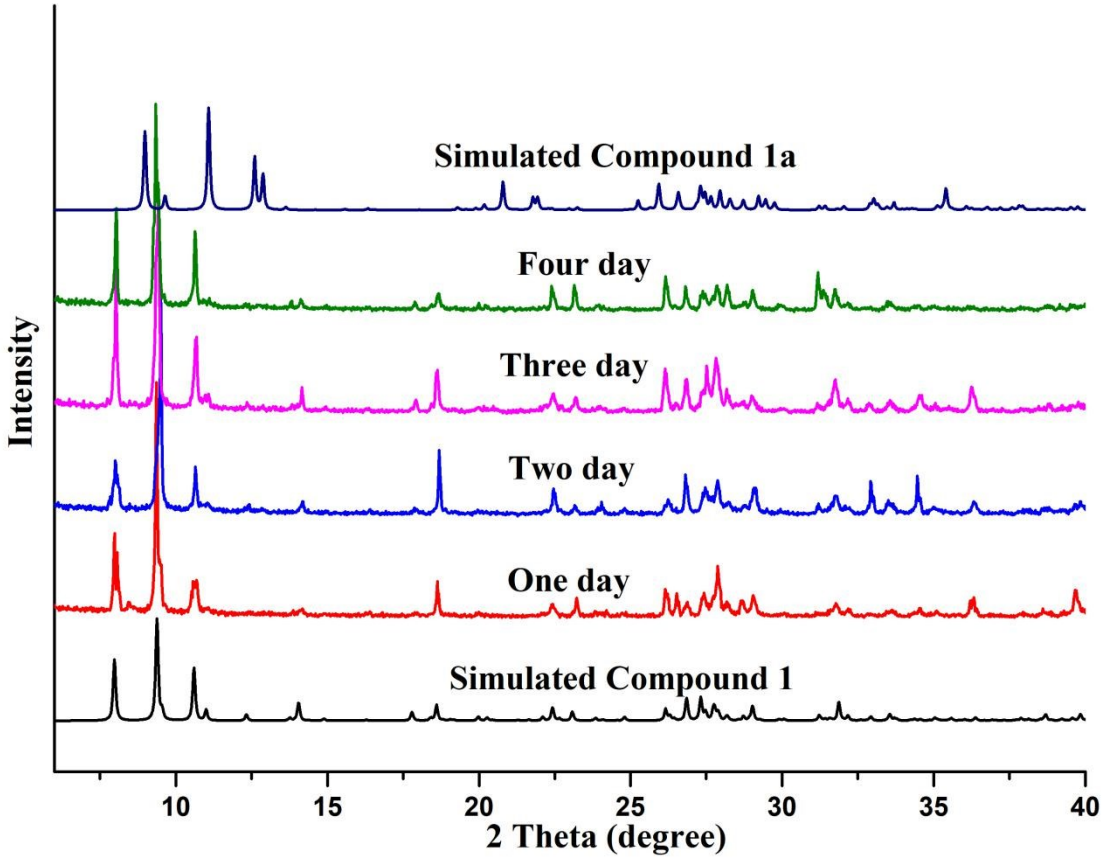

Fig. S16 Time-dependent PXRD patterns of Compound 1 soaked in toluene and simulated (black for Compound 1, dark blue for Compound 1a) PXRD patterns.

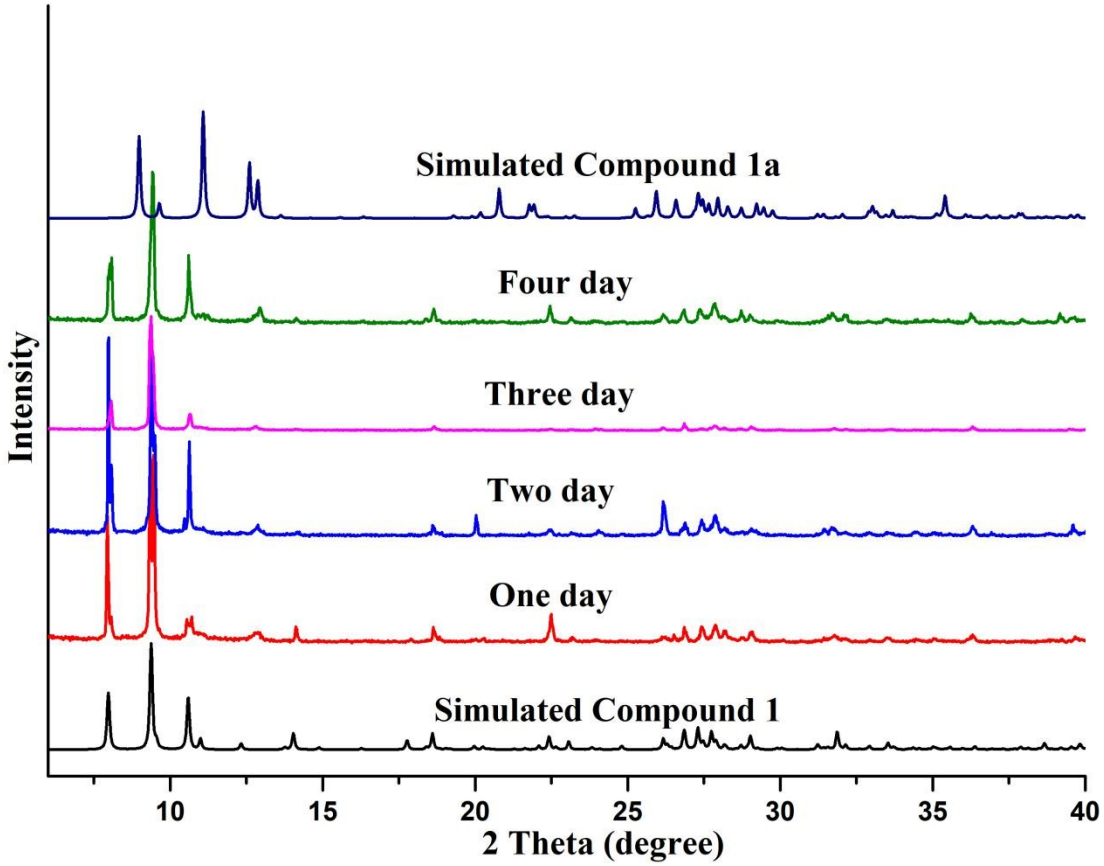

Fig. S17 Time-dependent PXRD patterns of Compound 1 soaked in dichloromethane and simulated (black for Compound 1, dark blue for Compound 1a) PXRD patterns.

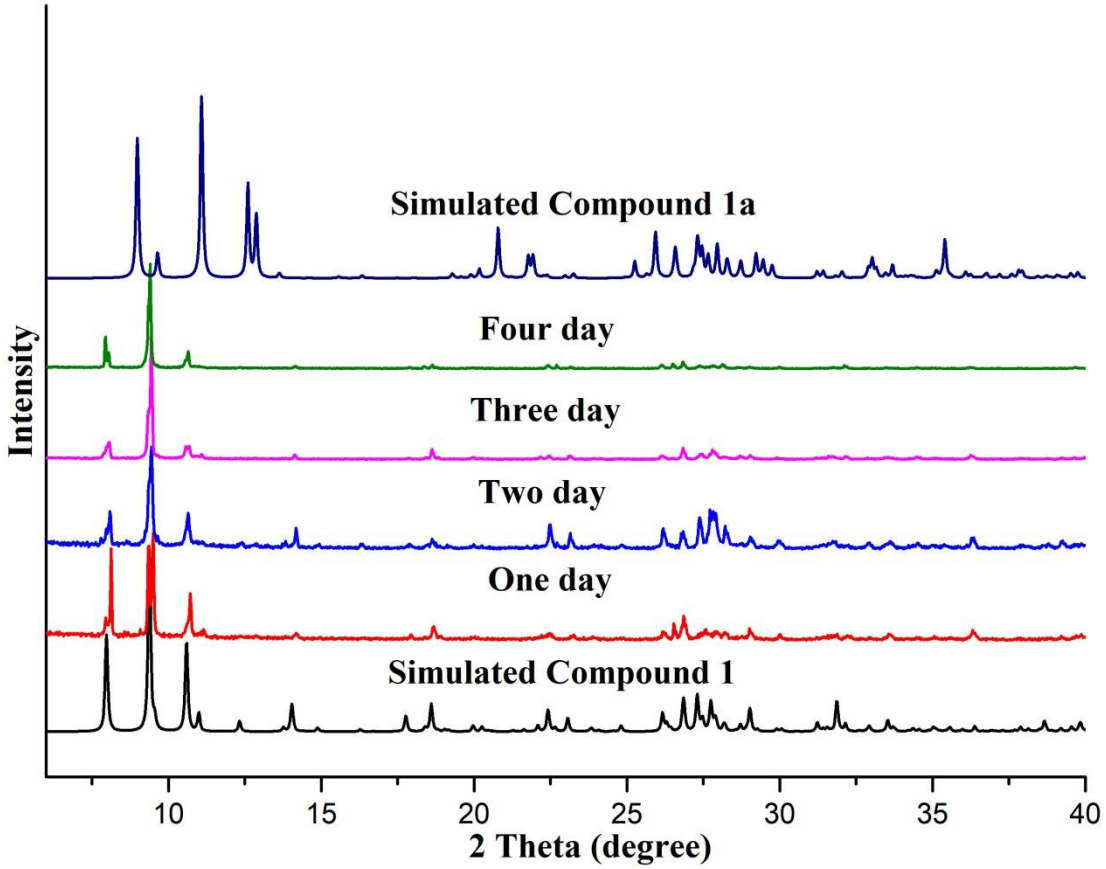

Fig. S18 Time-dependent PXRD patterns of Compound 1 soaked in N-hexane and simulated (black for Compound 1, dark blue for Compound 1a) PXRD patterns.

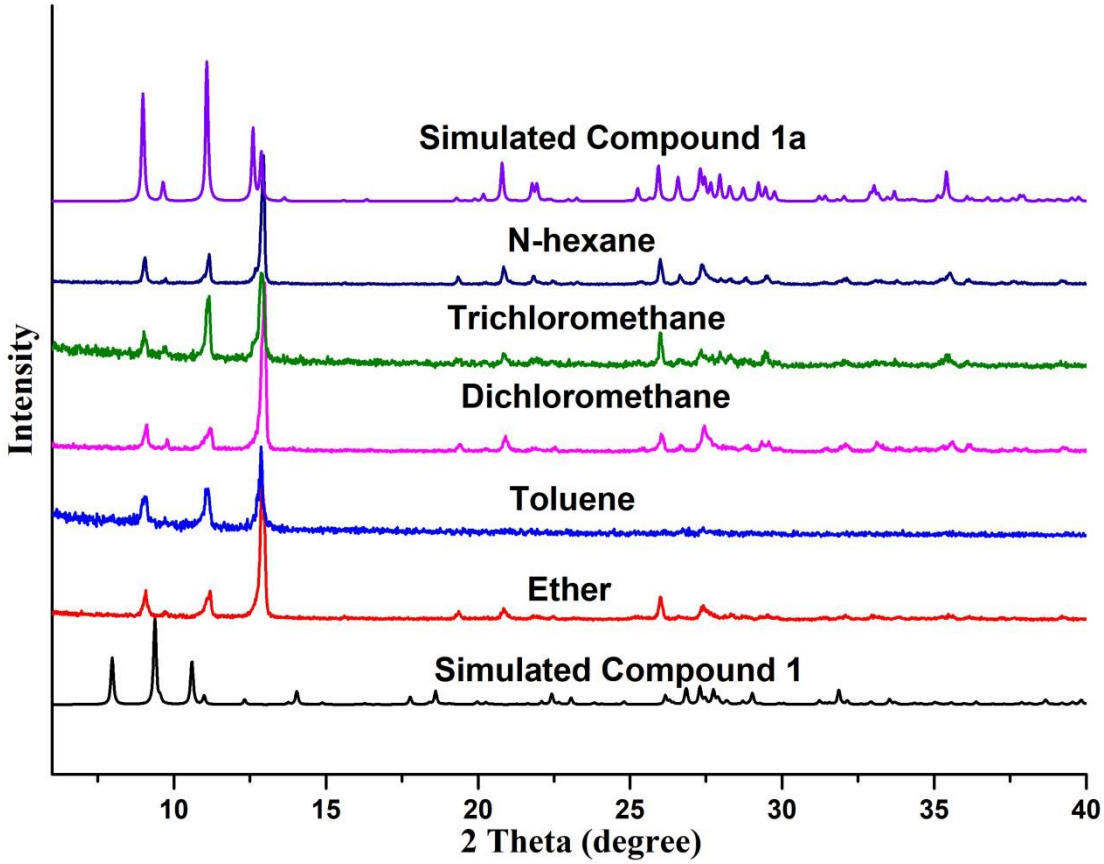

Fig. S19 Experimental (Compound 1 dry under the vacuum for 12 h after soaking in ether, toluene, dichloromethane, trichloromethane and N-hexane for 15 min) and simulated (black for Compound 1, purple for Compound 1a) PXRD patterns.

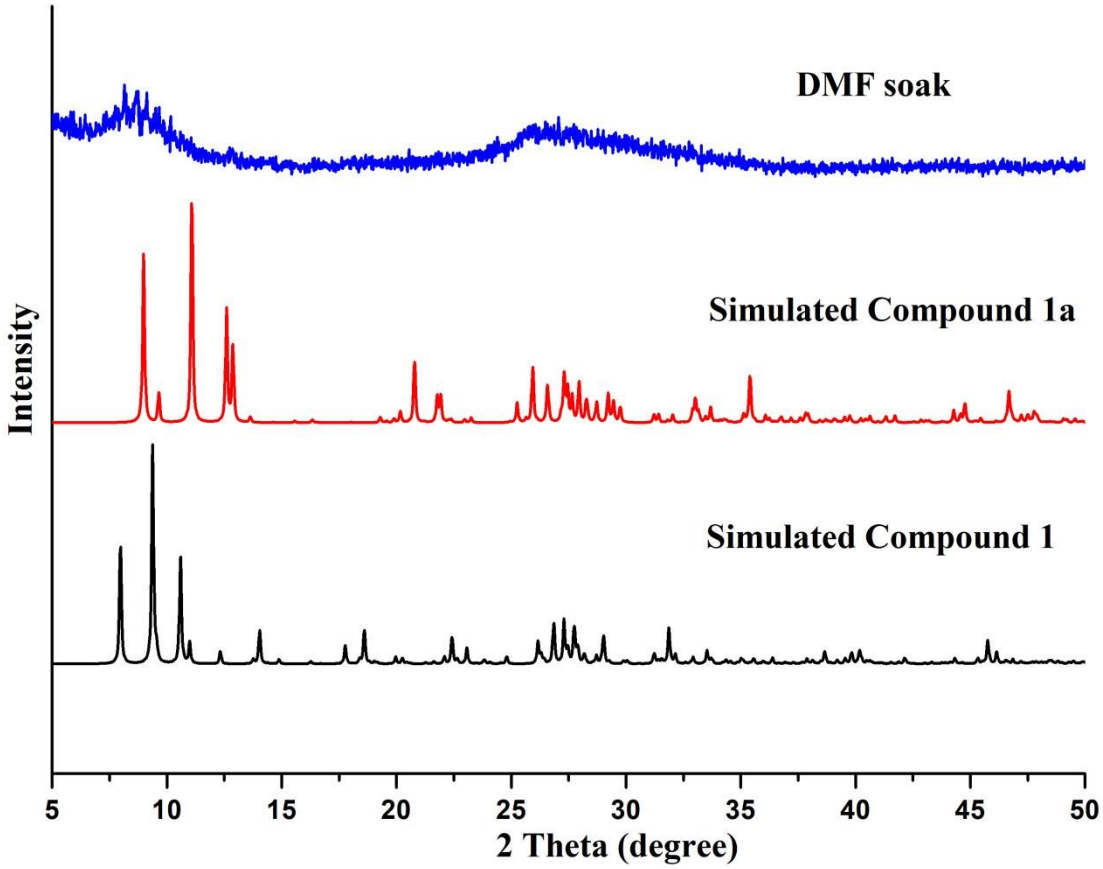

Fig. S20 Experimental (Compound 1 soaked in the DMF) and simulated (black for Compound 1, red for Compound 1a) PXRD patterns.

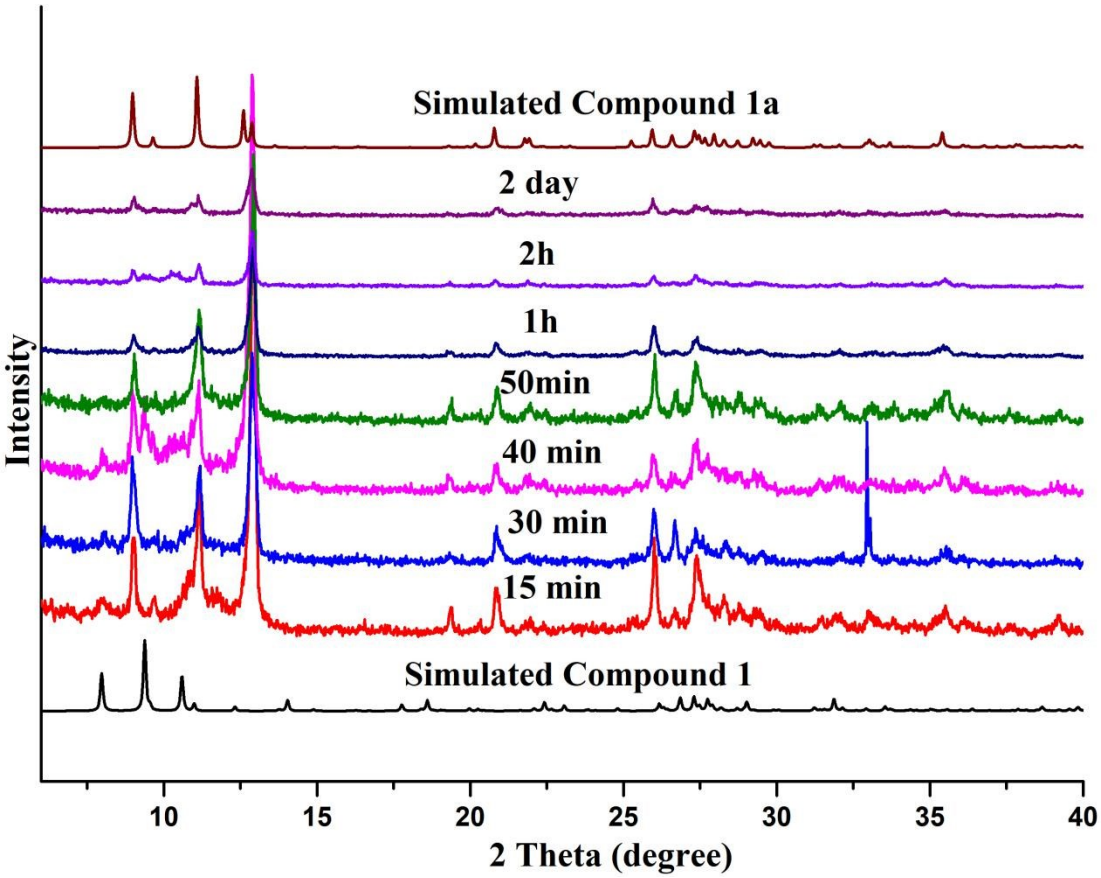

Fig. S21 Time-dependent PXRD patterns of Compound 1 soaked in methanol showing the transformation from Compound 1 to Compound 1a and simulated (black for Compound 1, brown for Compound 1a) PXRD patterns.

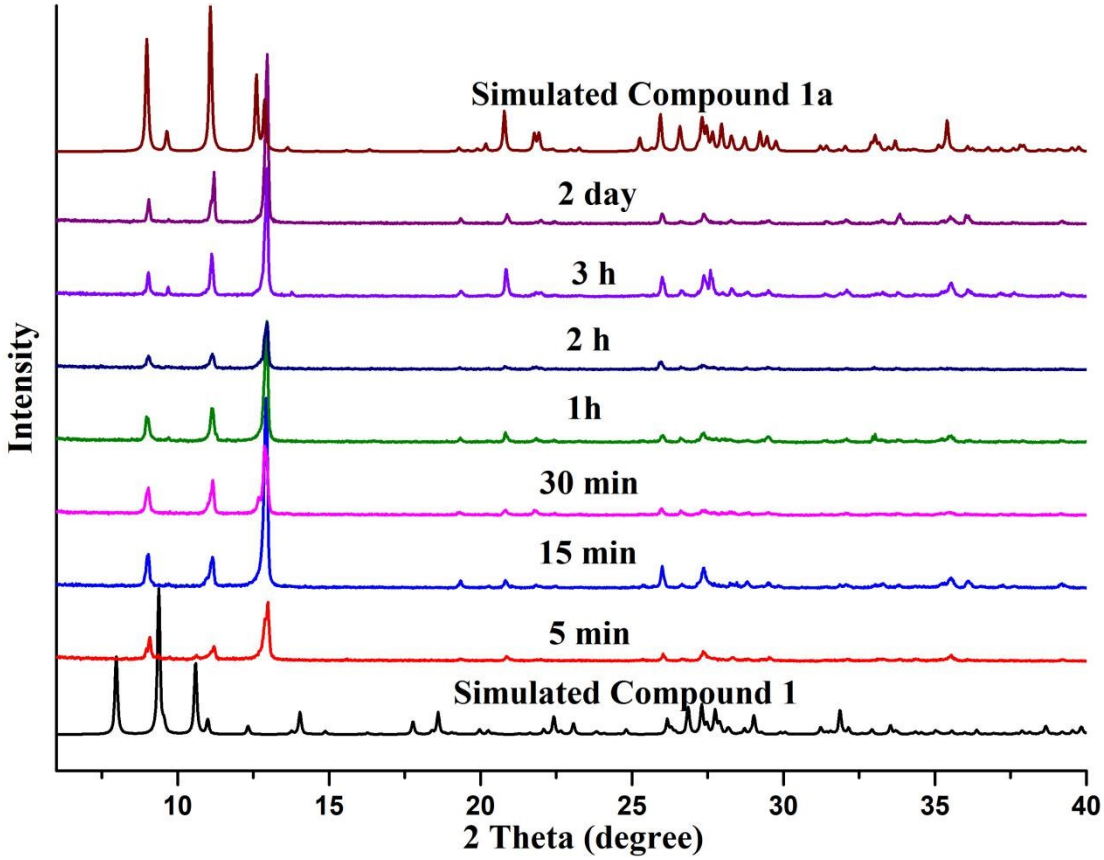

Fig. S22 Time-dependent PXRD patterns of Compound 1 soaked in ethanol showing the transformation from Compound 1 to Compound 1a and simulated (black for Compound 1, brown for Compound 1a) PXRD patterns.

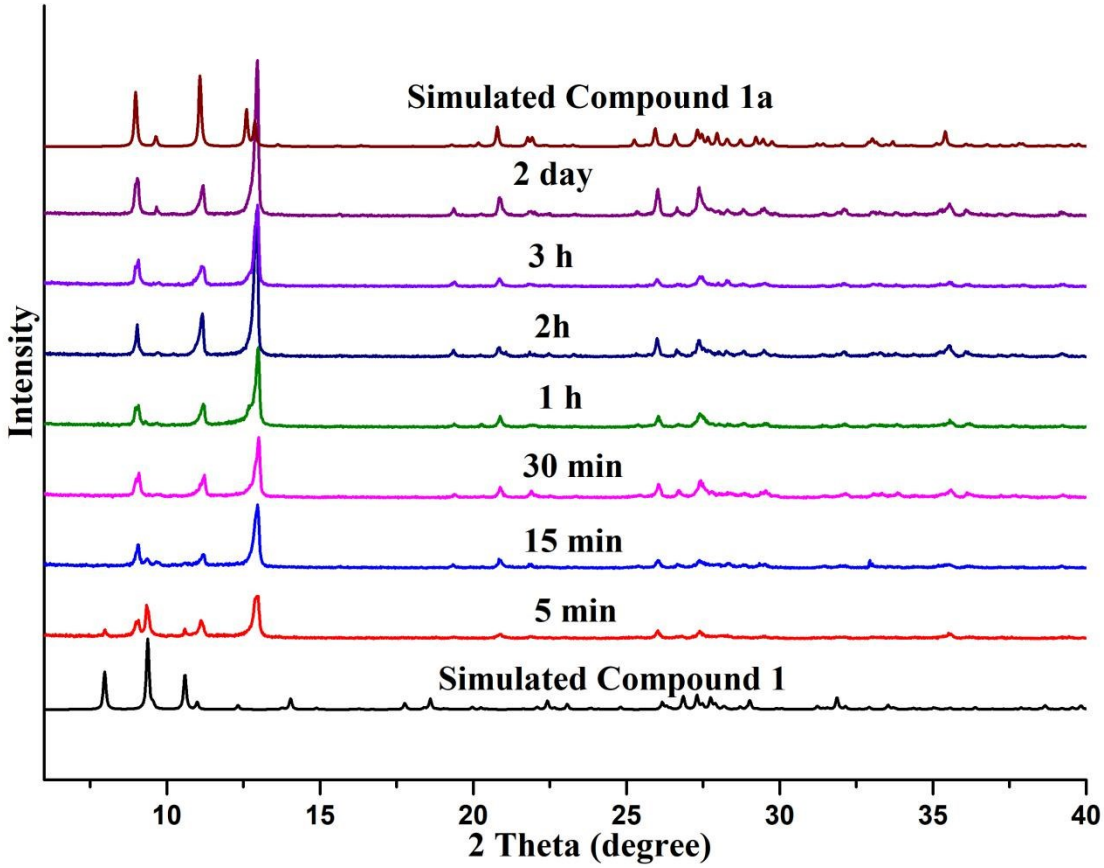

Fig. S23 Time-dependent PXRD patterns of Compound 1 soaked in acetonitrile showing the transformation from Compound 1 to Compound 1a and simulated (black for Compound 1, brown for Compound 1a) PXRD patterns.

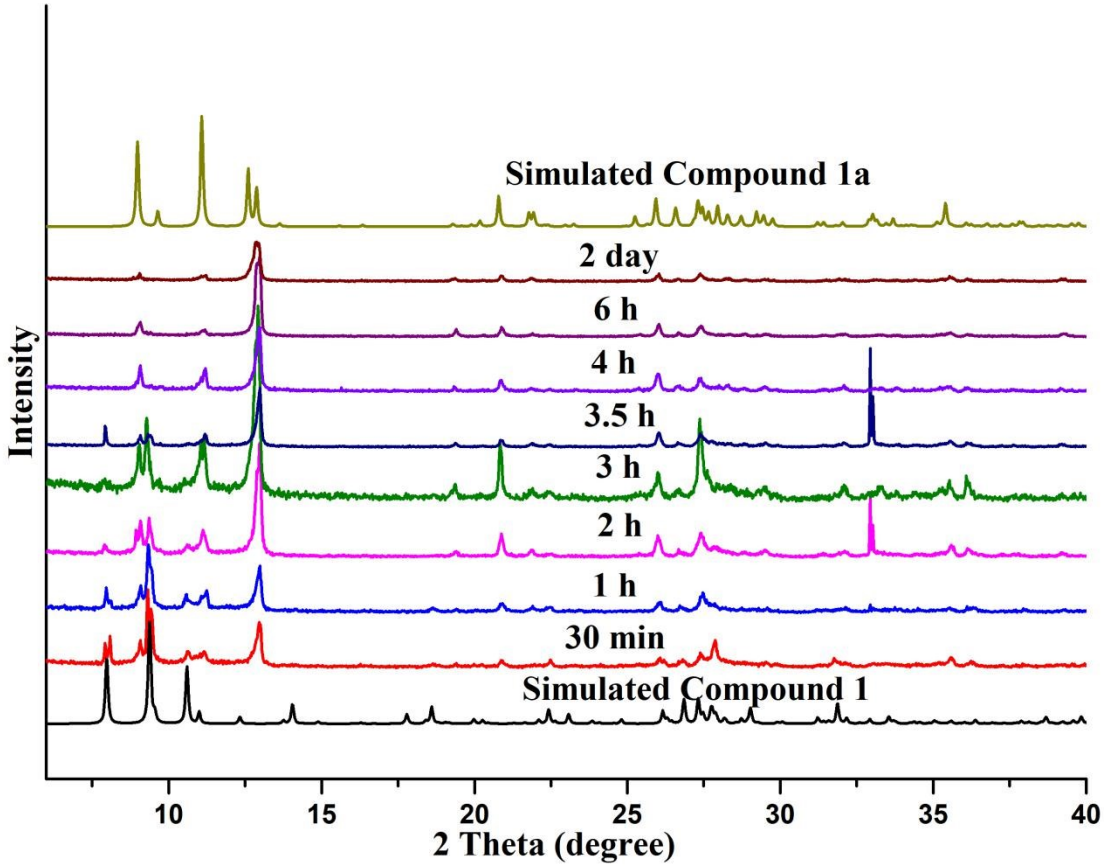

Fig. S24 Time-dependent PXRD patterns of Compound 1 soaked in THF showing the transformation from Compound 1 to Compound 1a and simulated (black for Compound 1, brown for Compound 1a) PXRD patterns.

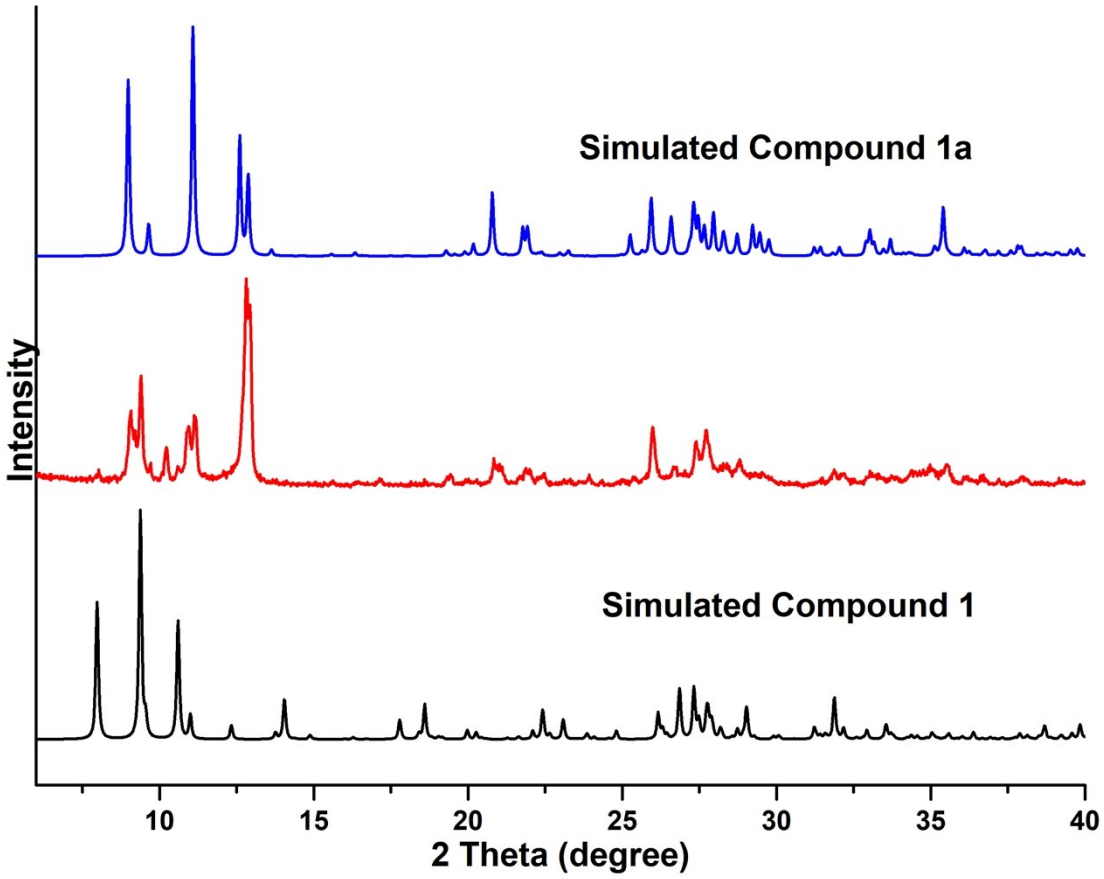

Fig. S25 Experimental (red for nanowires) and simulated (black for Compound 1, blue for Compound 1a) PXRD patterns.

S7 Thermogravimetric analyses (TGA)

Fig. S26 shows that the thermal decomposition process of Compound 1 and 1a can be divided into three steps. The first step corresponds to the remove of lattice water molecules, the second step refers to coordinated water, and the third step means the decomposition of the structure of polyanion framework. 15.4 % weight loss of compound 1 is comparable to fifteen lattice water molecules of Compound 1, while 6.3 % weight loss of Compound 1a means the removal of four lattice water molecules. The weight loss of second step for both compounds is 4.1 %, corresponding to four coordinated water molecules.

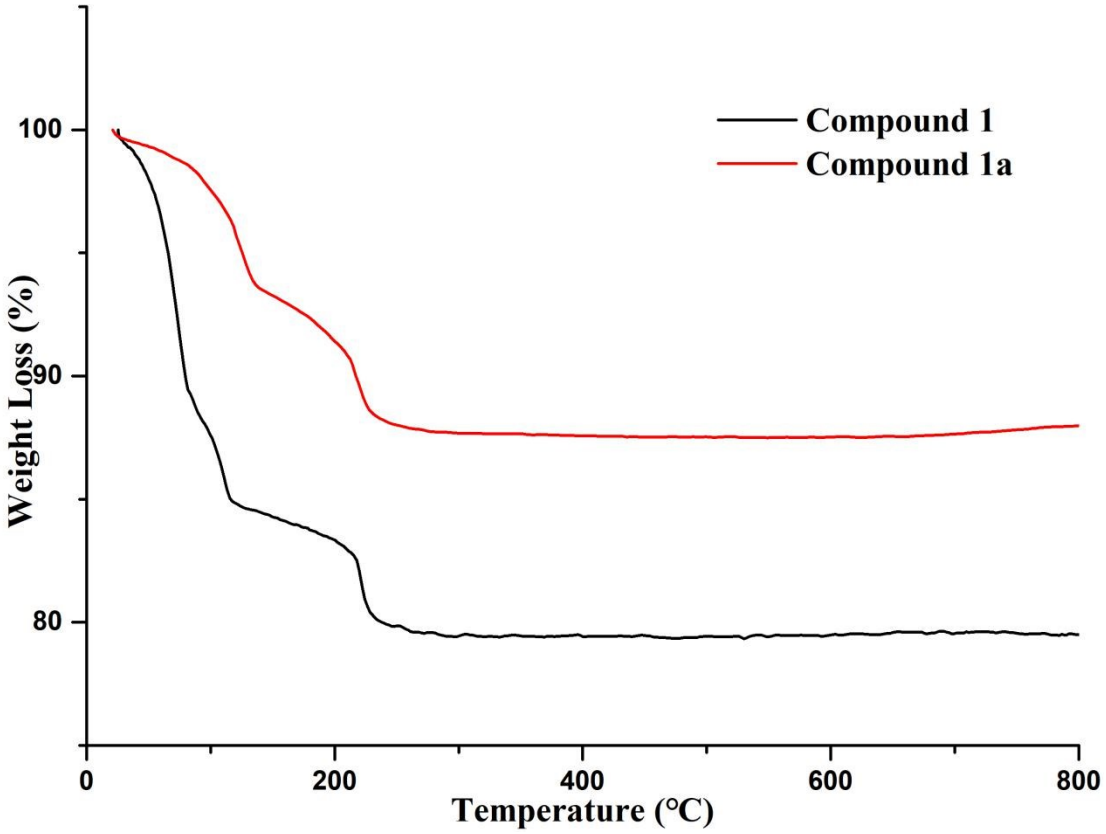

Fig. S26 The TGA curves of Compound 1 (black) and Compound 1a (red).

S8 UV-vis absorption spectrum

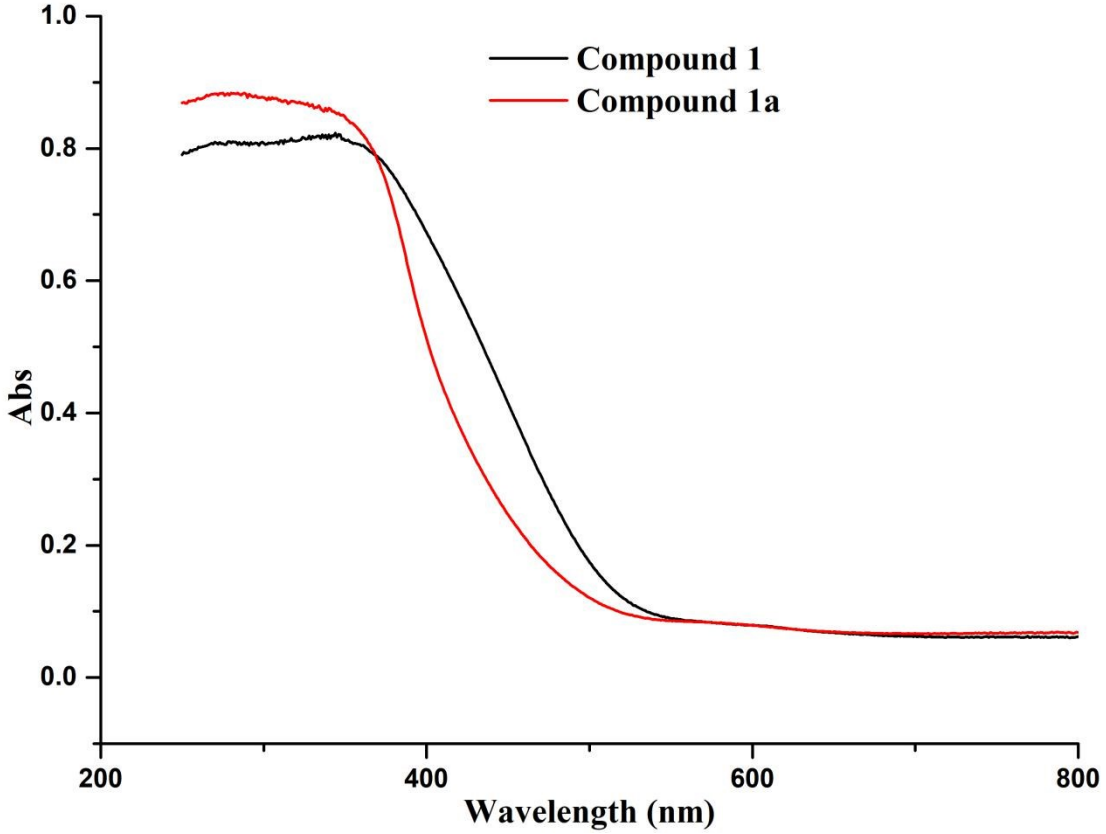

Fig. S27 Solid state UV-vis absorption spectrum of Compound 1 (black) and Compound 1a (red).

S9 SEM Measurement

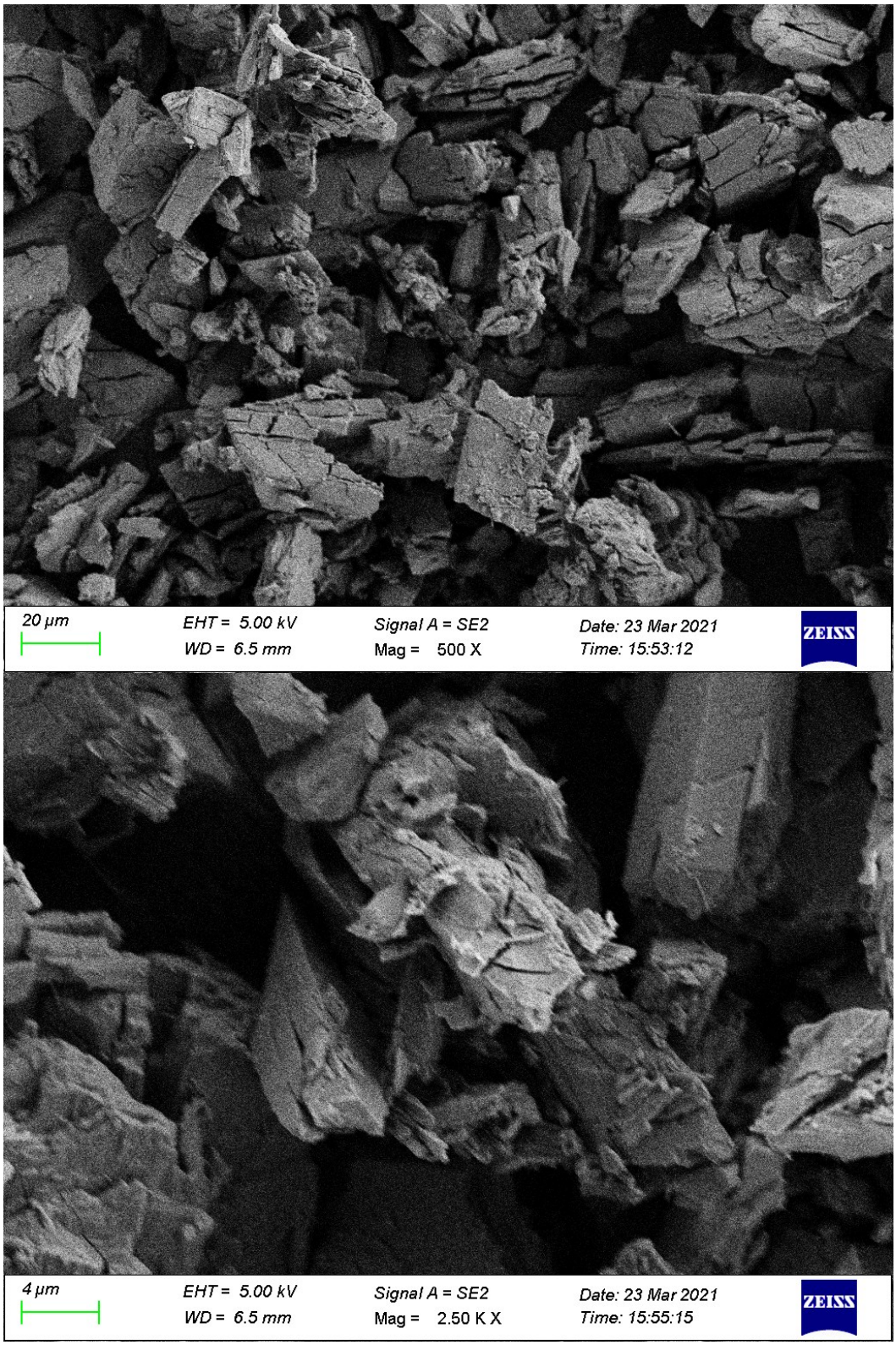

Fig. S28 SEM image of Compound **1** without treatment.

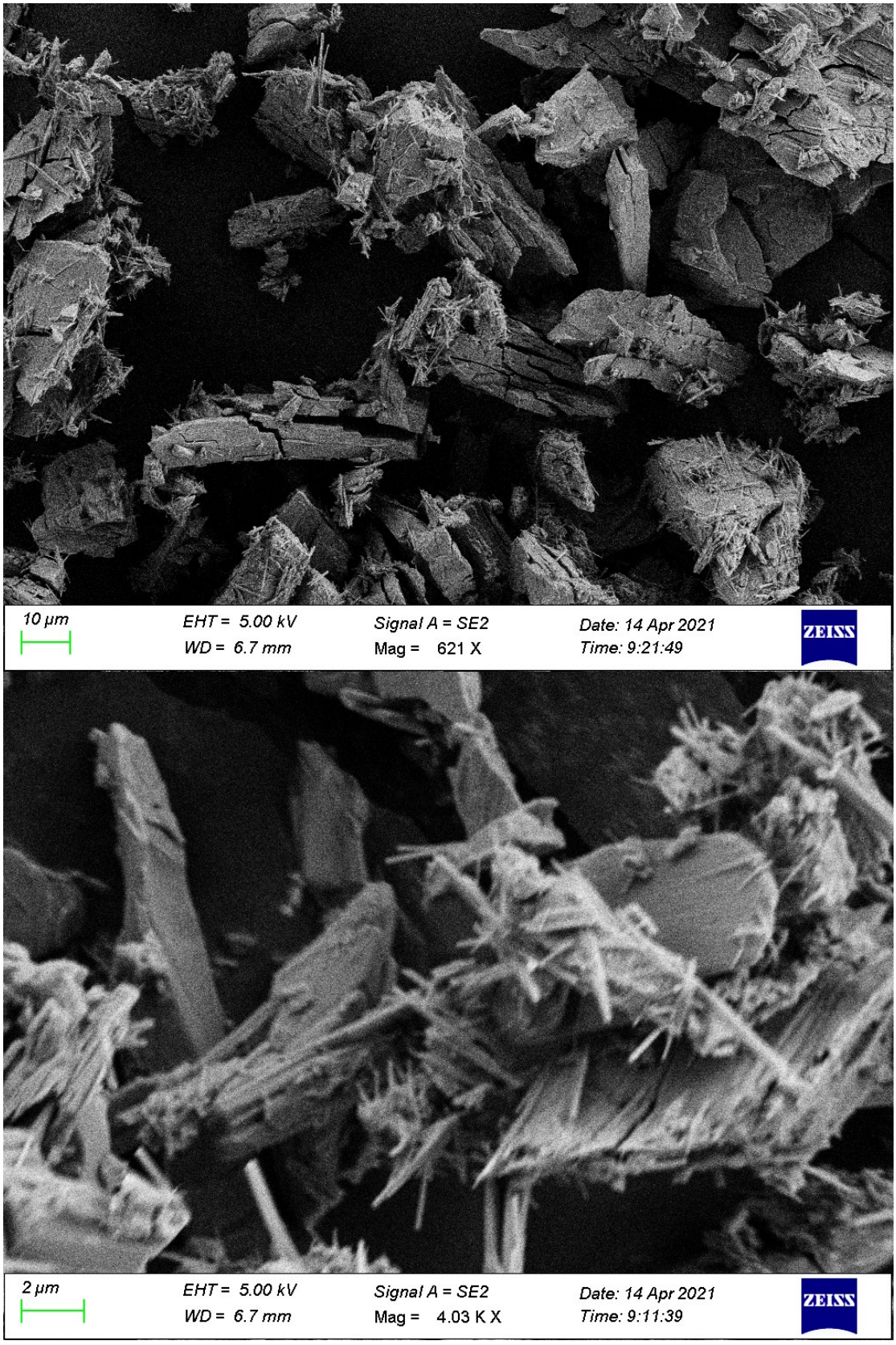

Fig. S29 SEM image of Compound **1** after vacuum drying for 12 hours.

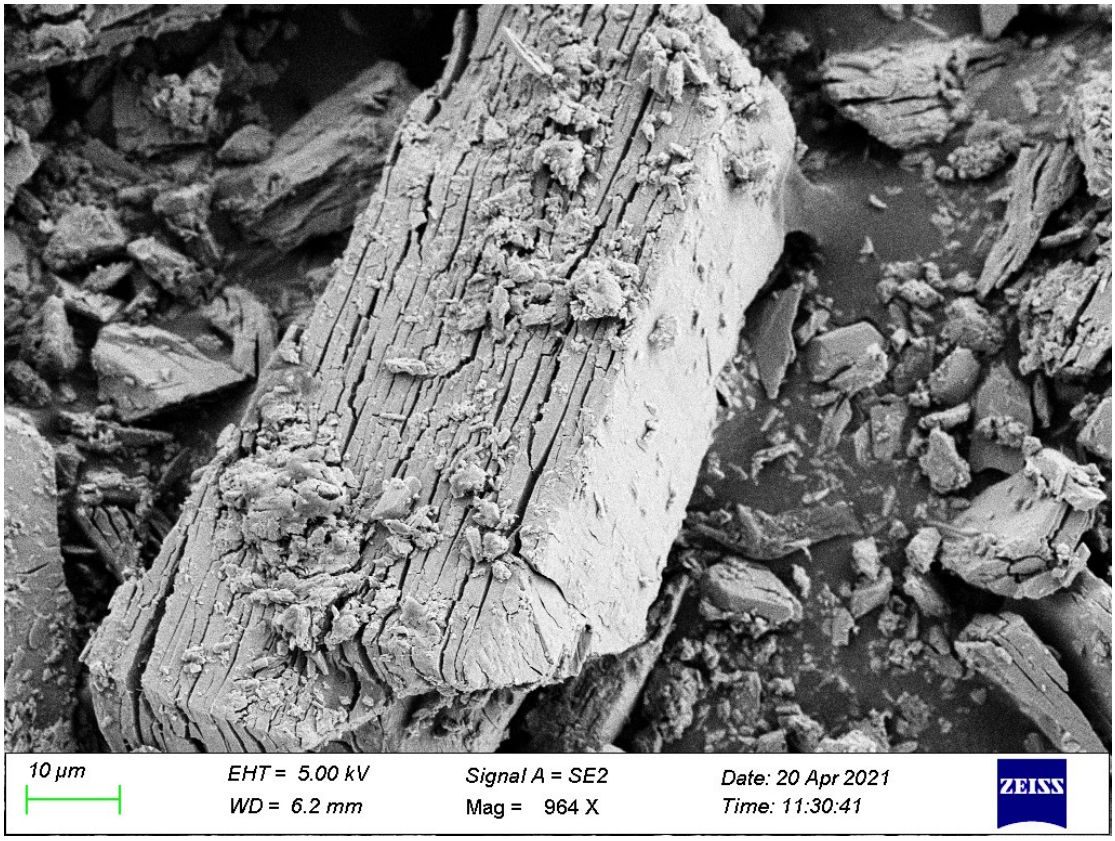

Fig. S30 SEM image of Compound **1** after grinding.

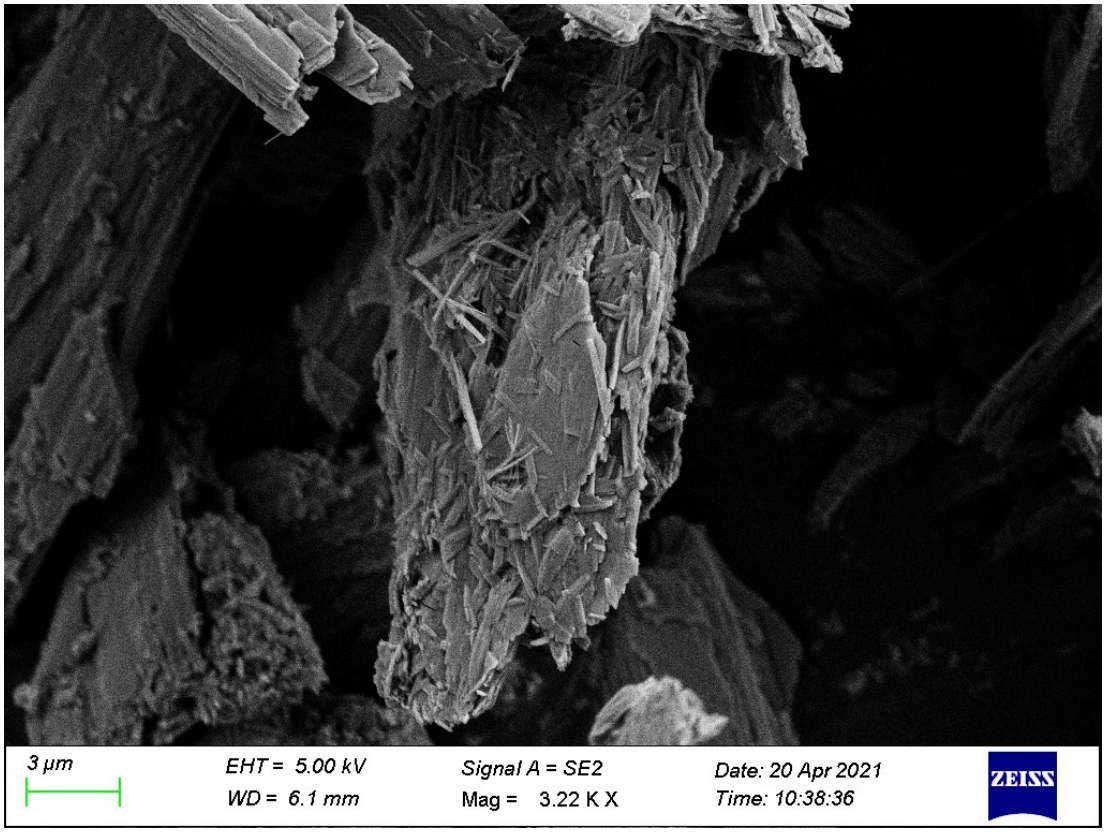

Fig. S31 SEM image of Compound **1** after soaking in CH_3OH.

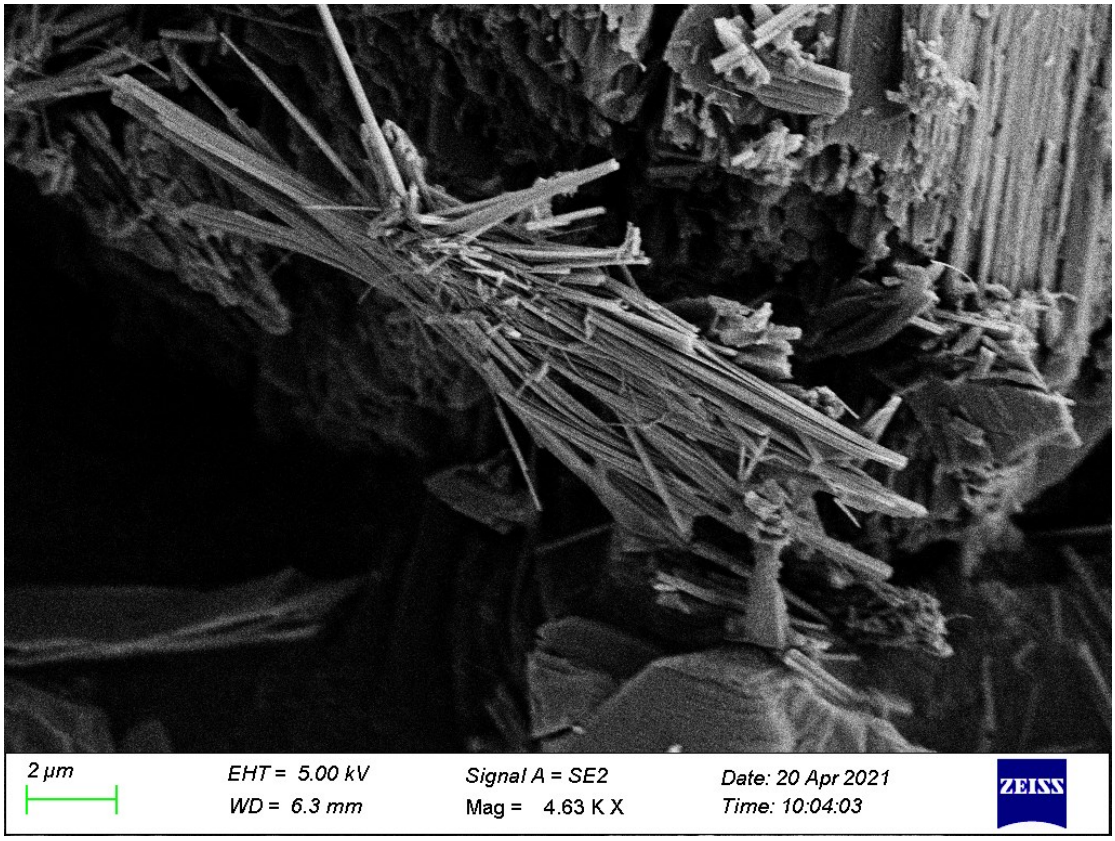

Fig. S32 SEM image of Compound **1** after soaking in C_2H_5OH.

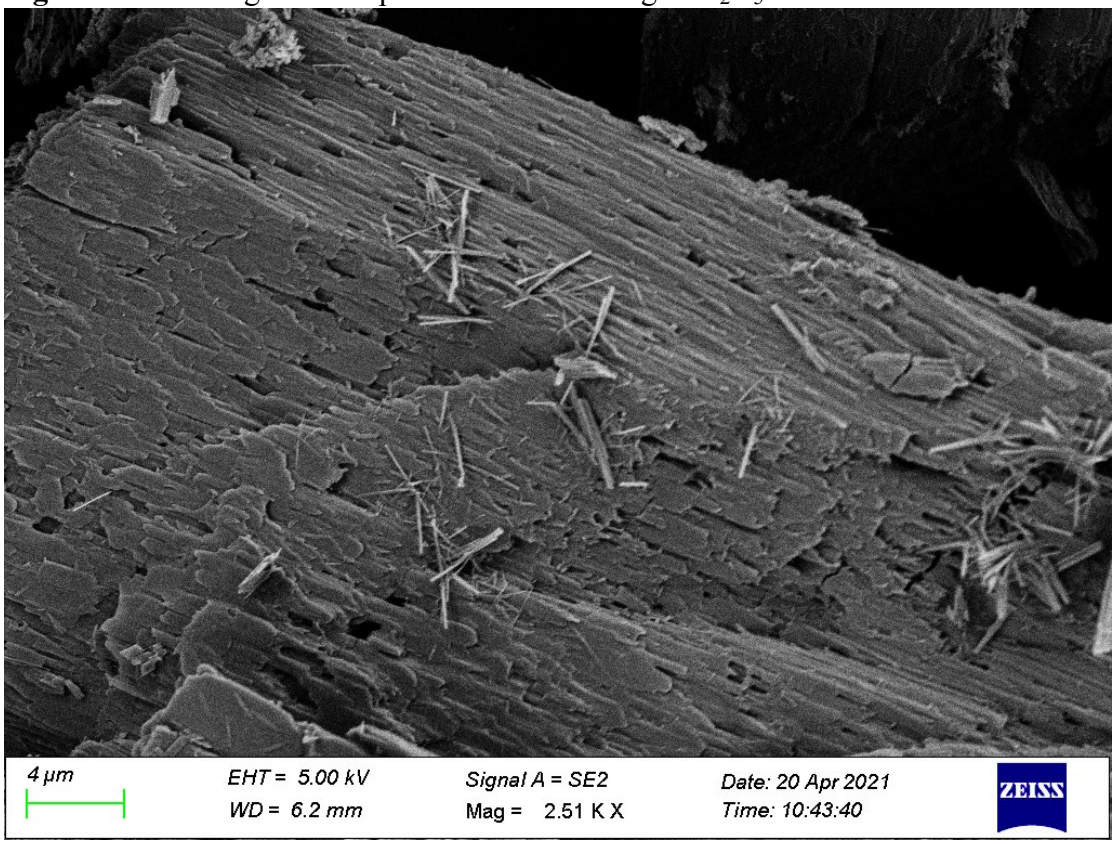

Fig. S33 SEM image of Compound **1** after soaking in CH_3CN.

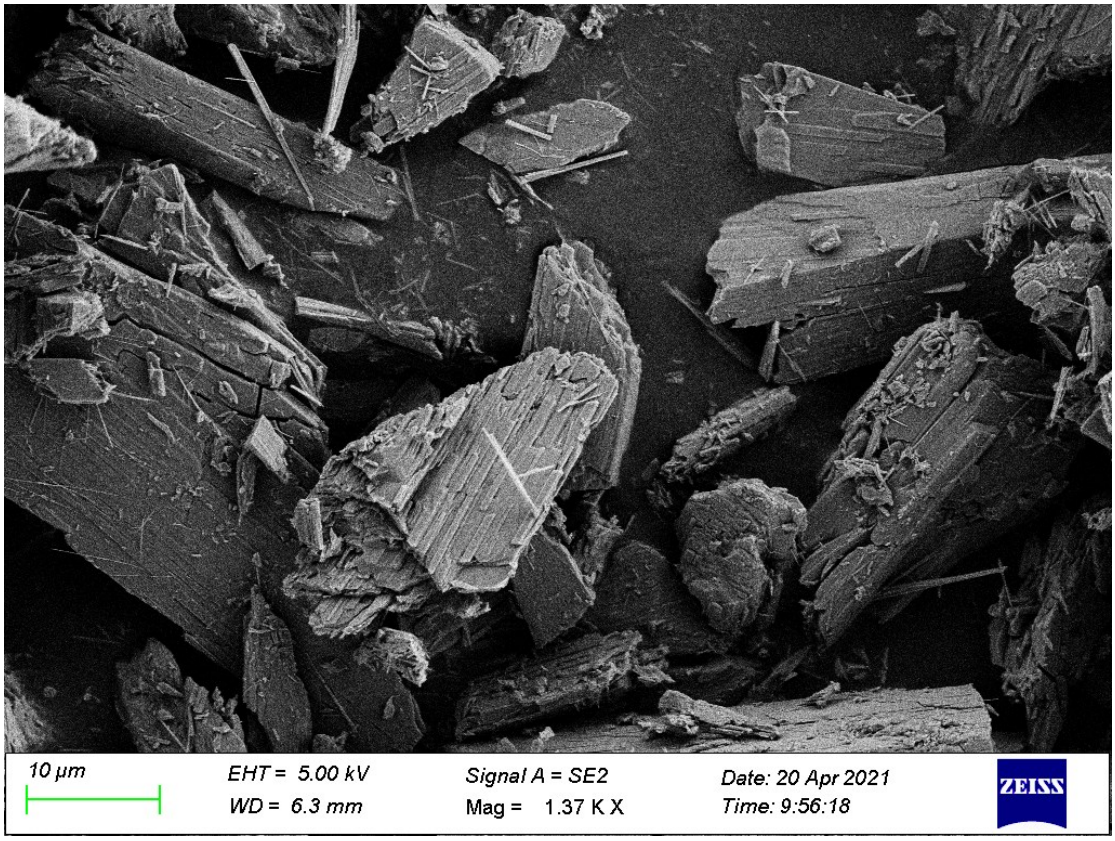

Fig. S34 SEM image of Compound **1** after soaking in THF.

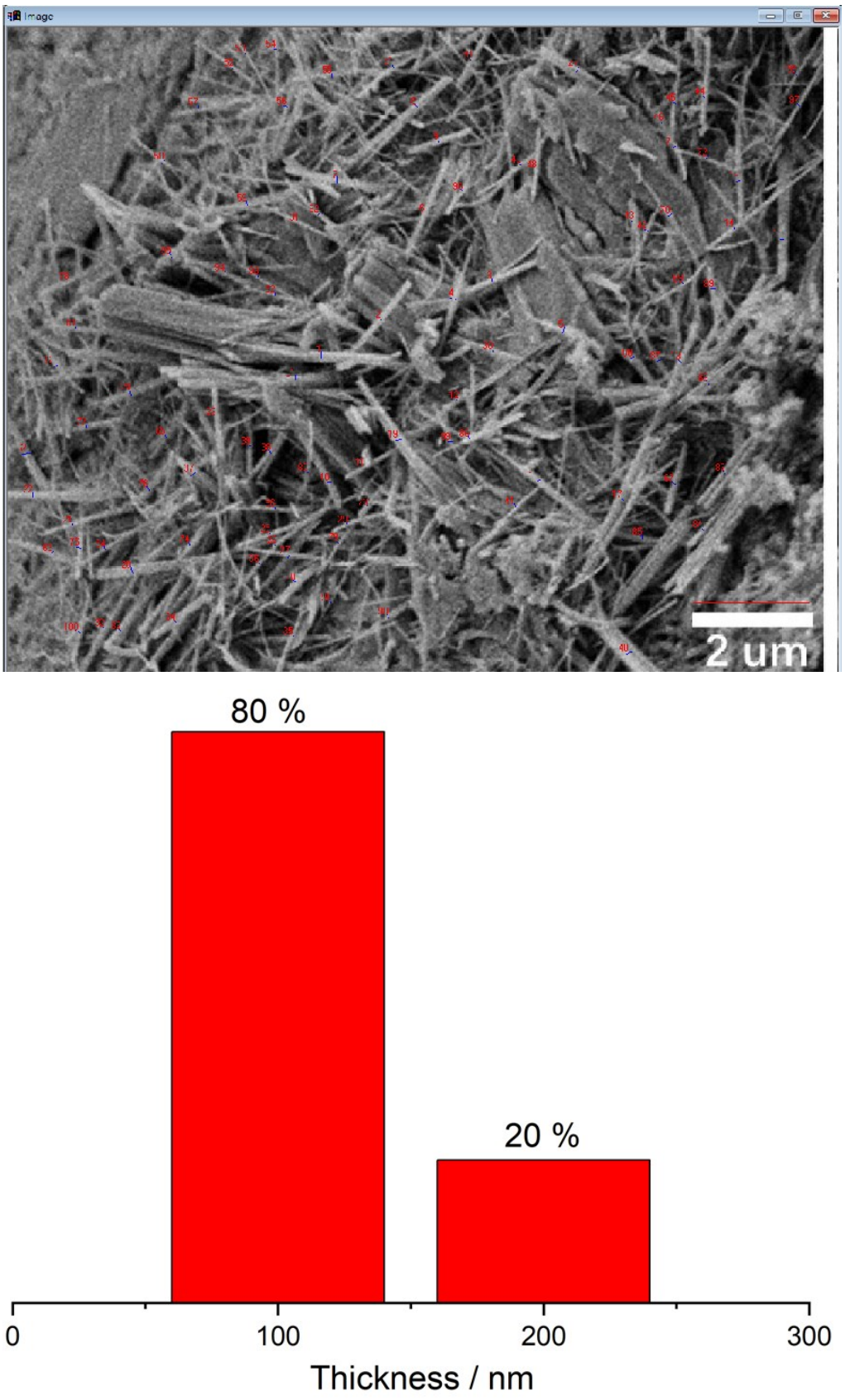

Fig. S35 Statistical distribution of nanowires in Compound 1a.

S10 Reference

1 Sheldrick, G. M. *Acta Cryst. A* **2008**, 64, 112.